PRESSURE LOSS OF WATER–CO_2 TWO-PHASE FLOW UNDER DIFFERENT OPERATING CONDITIONS

FARAJ BEN RAJEB[1], MOHAMMAD AZIZUR RAHMAN[2], YAN ZHANG[1], SYED IMTIAZ[1], AMER ABORIG[1] & MOHAMED ODAN[1]
[1]Faculty of Engineering & Applied Science, Memorial University of Newfoundland, Canada
[2]Texas A&M University at Qatar, Qatar

ABSTRACT

In the present study, pipe flows are used to investigate the behavior flow of water–CO_2 mixtures at different pressures and temperatures. The flow rate and pressure of water and CO_2 are changed by using a pump placed ahead of the mixing point. Pressure and temperature levels are recorded by pressure sensors and thermocouples affixed at points along the pipe loop. The flow regimes of two-phase water–CO_2 flow is visualized through transparent tubes using a high-speed camera. After several experiments, it was found that the mean pressure drop along the tube for a water–CO_2 system flow is about 4 kPa/m for water flow rates between 0.4 and 0.7 L/S and CO_2 flow rates between 2.5 and 11 L/S. The maximum inlet pressure for water is 400 kPa and for CO_2 is 3000 kPa. In this experiment, the phase fraction of water is approximately 0.5–0.15 and the phase fraction of CO_2 is around 0.85–0.95. The investigated flow regime under these flow conditions is often intermittent.

Keywords: carbon dioxide, water, two-phase flows, pressure loss, transportation.

1 INTRODUCTION

Global warming is considered the most challenging issue facing humanity today, with many research studies now focusing on investigating the main cause of this problem. Studying the behavior of carbon dioxide (CO_2) in its various phases can provide the key to resolving this critical issue. The wide range of CO_2 capture and storage (CCS) methods results in the transport of large quantities of CO_2 from the capturing locations to storage sites. The majority of these transportation processes occur through pipeline networks, where CO_2 can only be transported in a liquid or dense liquid state. This flow is usually a mixture of gas and liquid (i.e. a two-phase flow), although it sometimes contains impurities (i.e. a three-phase flow). Industrially, CO_2 is typically transported in a supercritical condition, which is a state between gas and liquid, with a density like a liquid and a viscosity like a gas. Transporting CO_2 by pipeline differs significantly from transporting natural gas via pipelines because CO_2 is often delivered in a dense liquid phase, whereas natural gas is transported in a dense gas state [1].

There are a number of challenges related to transportation of CO_2 through a pipeline. For instance, one study argues that because widespread applications of CCS need onshore CO_2 transport pipelines set up in populated areas [2], more safety guidelines are required due to pipeline pressure. At high concentrations, CO_2 is toxic and can cause unconsciousness almost instantaneously and respiratory arrest within one minute [3]. The carbon dioxide percentage is very low in normal room air (around 0.04%) [4], but at higher concentrations (>5%), toxicological effects begin in humans and animals. A carbon dioxide concentration of more than 10% may cause convulsions, coma and death, while concentrations of more than 30% can lead to loss of consciousness in seconds [3], [5]. In fact, even when CO_2 is transported in supercritical condition, water is present, along with nitrogen, oxygen, Sulphur oxides, methane, and other impurities [6].

This research also concluded that under normal transport conditions, a water level of 500 ppm is sufficiently low to minimize the risk of free water and hydrate formation. However, when CO_2 is transported above its critical pressure of 71.3 bar, the solubility of

WIT Transactions on Engineering Sciences, Vol 120, © 2018 WIT Press
www.witpress.com, ISSN 1743-3533 (on-line)
doi:10.2495/AFM180271

water is above 1300 ppm for a temperature range of -10°C to 25°C. In offshore pipelines, the temperature of the sea water is nearly always about 4°C. At this temperature, water solubility is above the proposed 500 ppm for pressures above 40 bars [1]. Based on these studies, CO_2 is always transported together with quantities of water at quantities that usually exceed the recommended ratio.

Other challenges reveal how the transport of CO_2 must be handled differently from the transport of oil and gas. One of these is that the critical point (7.38 MPa at 31.1°C) and triple point (about 518 kPa at -56.6°C) differ, which indicates that CO_2 is transported in a dense liquid state, whereas natural gas is transported in a dense gaseous state. Hence, most equipment and pipelines use for transporting natural gas are not suitable for transporting CO_2 [2].

In summary, previous studies recommended that when transporting CO_2 above supercritical condition, water content should be minimized to avoid corrosion and hydrate formation. However, when transported through pipelines in supercritical condition, CO_2 requires safer equipment design, especially in populated areas, in order to protect people against exposure to high concentrations of carbon dioxide. As a result, and for greenhouse applications, CO_2 needs to be transported at low pressure and with water moisture. In this work, we conduct an experiment to investigate the transporting of CO_2 in a gas phase at low pressure through a pipeline system.

2 THEORETICAL BACKGROUND

It is important to compare experimental results with theoretical calculations by using available empirical correlations. The Reynolds number is considered the most important parameter for flow regime estimations. In multiphase flows, mixing rules can be used to evaluate actual mixture properties such as density, viscosity, and velocity. The Reynolds number is also used in friction factor evaluations along with relative roughness, with the friction factor playing a role in pressure drop calculations.

2.1 Superficial velocities

2.1.1 Superficial velocity of liquid

$$U_{Ls} = \frac{q_L}{A}, \tag{1}$$

where A: cross-sectional area of flow (m); q_L: volume flow rate of liquid (m^3/s).

2.1.2 Superficial velocity of gas

$$U_{Gs} = \frac{q_G}{A}, \tag{2}$$

where q_G: volume flow rate of gas (m^3/s).

2.2 Mixture velocity

The sum of superficial velocities is called the mixture velocity:

$$U_{mix} = U_{Ls} + U_{Gs}. \tag{3}$$

2.3 Slip velocity

In general, gas and liquid tend to flow at different phase velocities in pipe flows.

The relative phase velocity or the slip velocity is defined by:

$$U_S = |U_G - U_L|. \tag{4}$$

The slip velocity is the ability of the phase which is less dense to flow at a greater velocity than the denser phase. We also can describe slip ratio (S) as:

$$S = \frac{U_G}{U_L}. \tag{5}$$

2.4 Phase fraction

The phase fraction of gas and liquid, λ, is defined as:

$$\lambda_L = \frac{q_L}{q_G + q_L}, \tag{6}$$

$$\lambda_G = 1 - \lambda_L, \tag{7}$$

where q_L and q_G are the volumetric flow rates of the two phases.

For a slip condition, we can define the true phase fraction for liquid and gas as:

$$\varepsilon_L = \frac{U_L}{U_L + \frac{1}{S}U_G}, \tag{8}$$

$$\varepsilon_G = \frac{U_G}{S.U_L + U_G}. \tag{9}$$

2.5 Two-phase mixing rule

Starting with the mixture density:

$$\rho_m = \rho_L \varepsilon_L + \rho_G \varepsilon_G, \tag{10}$$

the viscosity of gas-liquid mixture can be estimated from the Dukler correlation:

$$\mu_m = \varepsilon_G \mu_G + (1 - \varepsilon_G)\mu_L. \tag{11}$$

Now we can calculate the Reynolds number of the mixture, as follows:

$$Re_m = \frac{\rho_m u_m D}{\mu_m}. \tag{12}$$

2.6 Beggs and Brill method [7]

The Beggs and Brill correlation depends on the mechanical energy balance and in situ average density to determine horizontal flow regimes and calculate pressure gradient. In terms of horizontal flow regime estimations, the method depends on the Froude Number and other specific parameter calculations, as follows:

Froude Number:

$$N_{FR} = \frac{u_m}{\sqrt{gD}}, \tag{13}$$

$$\lambda_L = \frac{u_{SL}}{u_m}, \tag{14}$$

$$L_1 = 316{\lambda_L}^{0.302}, \tag{15}$$

$$L_2 = 0.0009252{\lambda_L}^{-2.4684}, \tag{16}$$

$$L_3 = 0.10\lambda_L{}^{-1.4516}, \tag{17}$$

$$L_4 = 0.5\lambda_L{}^{-6.738}. \tag{18}$$

The horizontal flow regimes used as correlating parameters in the Beggs and Brill approach are segregated, transition, intermittent, and distributed. The following gives the flow regime transitions.

Segregated flow exists if:

$$\begin{gathered}\lambda_L < 0.01 \ and \ N_{FR} < L_1 \quad or \\ \lambda_L \geq 0.01 \ and \ N_{FR} < L_2, \\ \lambda_L < 0.01 \ and \ N_{FR} < L_1 \quad or \\ \lambda_L \geq 0.01 \ and \ N_{FR} < L_2.\end{gathered} \tag{19}$$

Transition flow occurs when:

$$\lambda_L \geq 0.01 \ and \ L_2 < \quad N_{FR} \leq L_3. \tag{20}$$

Intermittent flow exists when:

$$\begin{gathered}0.01 \leq \lambda_L < 0.4 \ and \ L_3 < N_{FR} \leq L_1 \ or \\ \lambda_L > 0.4 \ and \ L_3 < N_{FR} \leq L_4.\end{gathered} \tag{21}$$

Distributed flow occurs if:

$$\begin{gathered}\lambda_L < 0.4 \ and \ N_{FR} \geq L_1 \ or \\ \lambda_L \geq 0.4 \ and \ N_{FR} > L_4.\end{gathered} \tag{22}$$

Pressure drop calculations:

$$P_{tf} = P_1 + \Delta P_L + \Delta P_f, \tag{23}$$

where P_{tf} = Pressure flowing at any location in the pipeline (kPa).; P_1 = Pressure at the tubing loop starting-point before two-phase mixing (kPa); ΔP_L = Pressure drops through the flow line (kPa); ΔP_f = Pressure drops through the fittings (kPa)

$$\Delta P_L + \Delta P_f = f\left(\frac{L}{D} + \sum \frac{L_e}{D}\right)\frac{\rho v^2}{2g}. \tag{24}$$

3 EXPERIMENTAL MEASUREMENTS

A multiphase pipe flow loop was used to investigate water–CO_2 flow and to record the flow conditions. The experiments took place at Memorial University in Newfoundland, Canada. The experimental results in this study were compared with theoretical calculations, while the flow regime of gas/liquid flow was investigated and compared with available flow regimes. The pressure loss along pipelines, recorded by sensors, was verified with models.

The experiment starts with the flow of gas and liquid from a CO_2 cylinder and water tank, respectively. The water tank is connected to a high-pressure multiphase pump that pushes water to the network pipelines. The mixing point of water and CO_2 occurs at the beginning of the pipeline loop. Several pressure sensors and thermocouples are fixed at specific points on the loop. In addition, gas and liquid flowmeters are installed ahead of the mixing point to record CO_2 and water flow rates individually. In order to read the results, all of the pressure sensors and thermocouples are connected to a data acquisition system linked to a computer.

The experimental procedure continues with the addition of fixed water velocity. The gas velocity is then increased three times towards higher velocity, with flow conditions recorded each time. The velocity of the CO_2 can be changed via the valve and regulator on the CO_2 cylinder. The next step is raising the water velocity by increasing the inlet pump pressure and changing the gas velocity several times at the same water velocity. Following this step, the velocity of the gas and liquid are altered several times and the flow type that results from the flow regime of the mixture flow is investigated. The pressure drops along the pipeline are recorded and saved on the computer.

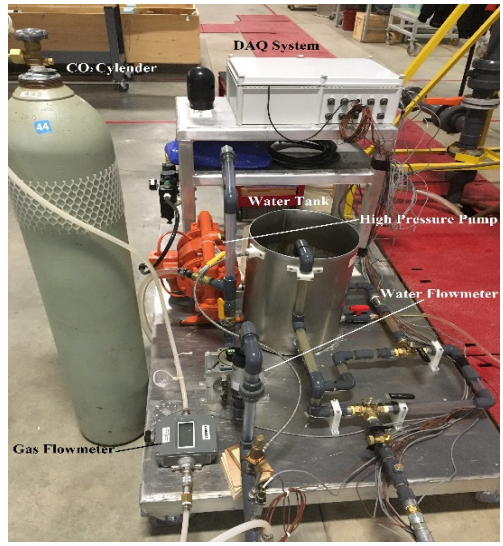

Figure 1: Experimental set-up of the fluid supply section.

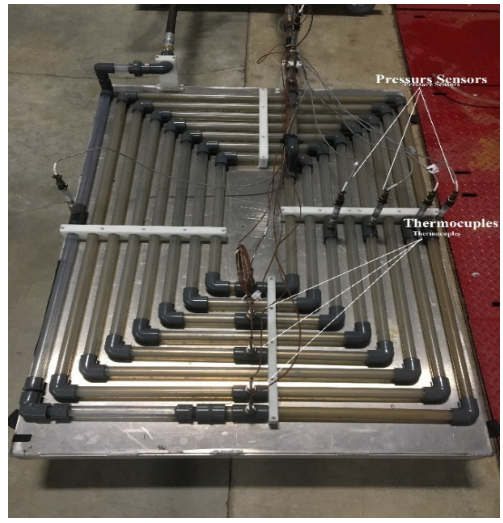

Figure 2: Experimental set-up of the flow loop test section.

4 RESULTS AND DISCUSSION

4.1 Impact of water on flow pressure

When gases are flowing in a pipeline, pressure flow can be difficult to maintain. The pressure drops rapidly to less than atmospheric pressure when there is a decrease in gas flow rate and CO_2 gas flowing through pipes. However, by mixing water with CO_2 in a pipe flow, we can maintain the flow pressure and thus increase the volume of the CO_2 delivered.

Table 1 shows the overall flow loop pressure drop and the pressure after traveling along a 3 m length of tube versus a CO_2 flow rate for a single-phase flow (for CO_2 only). Table 2 shows the same data for a water–CO_2 flow.

Table 2 explains the difference in pressure values after 3 m from the starting flow on the tubing system when CO_2 is flowing alone and as a mixture with water. It is clear that when water flows with CO_2, we can achieve a flow pressure more than 20 times higher than that of the CO_2 flow.

Fig. 3 also compares CO_2 flow and water–CO_2 mixture flow in terms of pressure drop for overall length of tube.

4.2 Phase fraction

Fig. 4 shows how phase fractions change by changing the velocities of both phases. This figure illustrates the relationship between gas phase fraction and slip ratio at different liquid flow rates. The slip ratio increases when the gas fraction increases and the flow rate of gas increases. We can also see that the velocity of water does not have as large an impact on slip ratio as CO_2. Therefore, we can say that the slip ratio is more affected by the velocity of CO_2 than the velocity of water.

Table 1: Experimental pressure drop and pressure for CO_2 flow.

Gas flow (L/S)	ΔP (kPa)	Pressure at 3 m pipe length (kPa)
5	9	11
8	10	12
9	12	15
10	14	16
11	21	24

Table 2: Experimental pressure drop and pressure for water–CO_2 flow.

Gas Flow (L/S)	ΔP (kPa)	Pressure at 3 m pipe length (kPa)
4	158	230
8	205	294
9	227	356
10	276	445
11	285	455

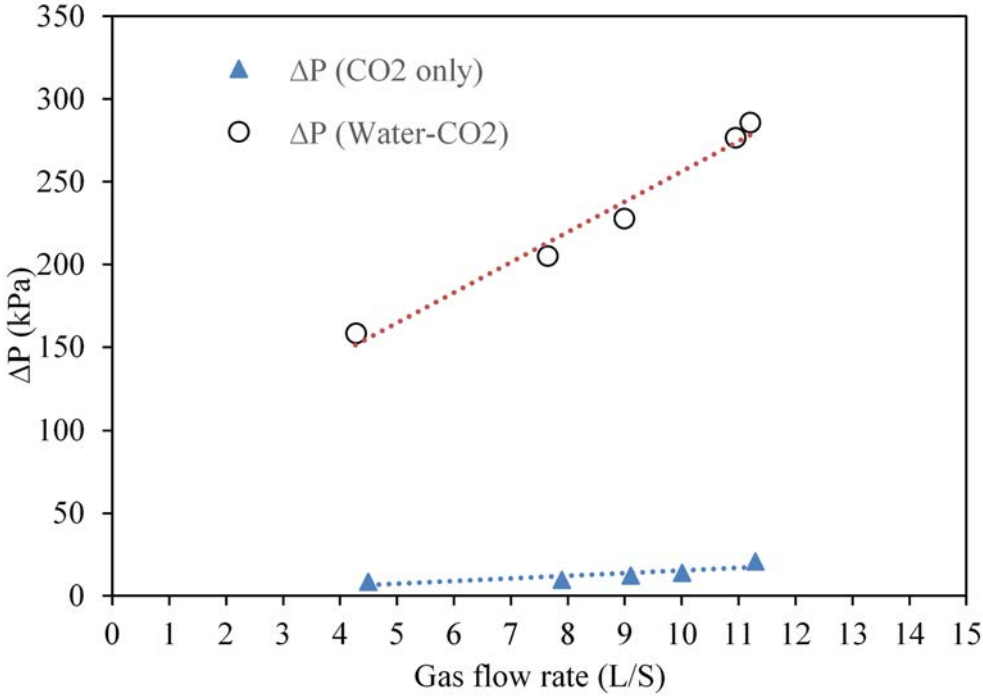

Figure 3: Comparing pressure drop vs. gas flow rate for CO_2 flow and water–CO_2 flow.

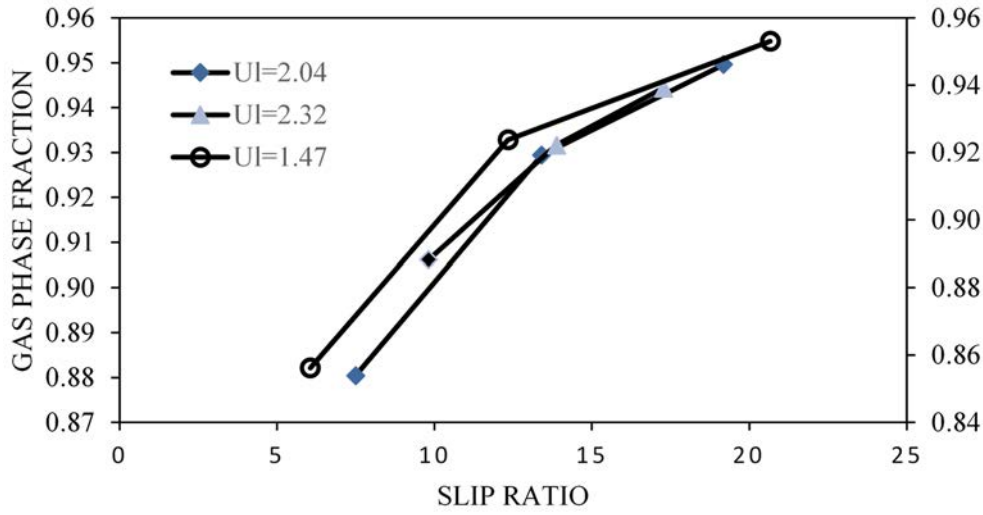

Figure 4: Relationship between slip ratio U_G/U_L and gas phase fraction for water–CO_2 flow.

Table 3: Slip ratio and phase fraction at different velocities of gas and liquid.

U_L (m/sec)	u_g (m/sec)	S (u_g/u_l)	Liquid phase fraction	Gas phase fraction
1.47	8.93	6.06	0.14	0.86
1.47	18.18	12.33	0.08	0.92
1.47	30.46	20.66	0.05	0.95
2.04	15.25	7.49	0.12	0.88
2.04	27.29	13.40	0.07	0.93
2.04	39.07	19.19	0.05	0.95
2.32	22.75	9.82	0.09	0.91
2.32	32.14	13.87	0.07	0.93
2.32	40.00	17.27	0.06	0.94

4.3 Pressure gradient

Fig. 5 depicts experimental and theoretical overall pressure drops at different gas and liquid flow rates compared with pressure drops calculated by available correlations versus Reynold number for water CO_2 flow.

According to Fig. 5, the pressure drop recorded in the experiment is nearly the same as the pressure calculated in eqn (24). Table 4 shows the percentage error between experimental and theoretical pressure drops.

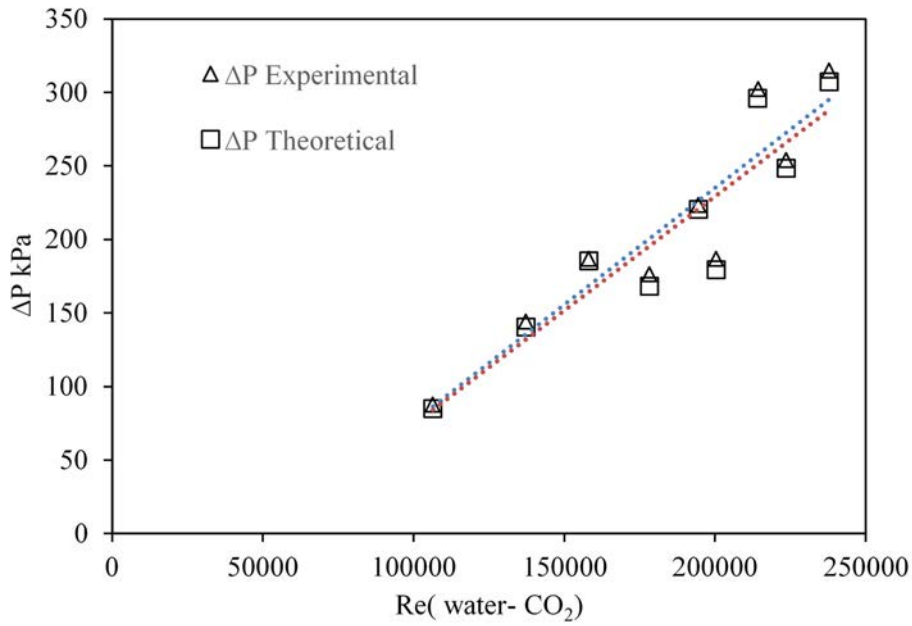

Figure 5: Pressure drop experimentally and theoretically versus Reynolds number for water–CO_2 flow.

Table 4: Comparison of experimental and theoretical pressure drops for water–CO_2 flow.

ΔP Ex kPa	ΔP Cal kPa	ΔP Error %
87.85	85.08	3.15
144.28	140.42	2.67
186.99	185.61	0.74
176.38	168.29	4.59
223.44	220.40	1.36
302.33	296.13	2.05
186.79	179.32	4.00
254.17	248.48	2.24
314.94	307.20	2.46

4.4 Flow regime

The flow regime of the two-phase flow is investigated while the experiment is running. Transparent tubes are used to determine the flow type. In addition, the Beggs and Brill correlation [8] is used to estimate the flow regime of the water–CO_2 flow. Tables 5 and 6 show the method used to calculate the estimation of the flow regime.

As can be seen from Table 6, the flow type is always intermittent, which is the same as in the experimental system. This flow regime is confirmed for a range of CO_2 velocities between 8 and 40 m/sec and water velocities between 1 and 3 m/sec, flowing in a tube measuring ¾ inches 0.01905 m in diameter.

Table 5: Reynolds and Froud Numbers for water–CO_2 flow vs. mixture velocity.

U_m(m/s)	Re=ρuD/μ	NFR=U_m^2/Dg
10.40	106,600.56	24.06
19.65	137,231.00	45.46
31.94	157,994.79	73.88
17.29	159,886.96	39.99
29.32	194,318.68	67.83
41.11	214,248.56	95.09
25.07	200,396.43	57.99
34.46	223,373.01	79.71
42.32	237,282.40	97.89

Table 6: Beggs and Brill factors vs. concluded flow regime for water–CO_2 flow.

λ_L	L_1	L_2	L_4	L_3	NFR	Flow regime
0.14	175	0.12	111	1.71	24.06	Intermittent
0.07	144	0.55	649	4.29	45.46	Intermittent
0.04	124	1.83	2,490	8.69	73.88	Intermittent
0.11	165	0.18	186	2.23	39.99	Intermittent
0.06	141	0.67	804	4.80	67.83	Intermittent
0.04	127	1.54	2,049	7.84	95.09	Intermittent
0.09	153	0.33	364	3.17	57.99	Intermittent
0.06	139	0.72	879	5.03	79.71	Intermittent
0.05	131	1.20	1,552	6.78	97.89	Intermittent

4.5 Dimensionless number trends

The values of Reynolds and Froude numbers were estimated for a range of gas and liquid velocities. As is known, the Reynolds number is the ratio of inertial forces to viscous or frictional force, while the Froude Number refers to the ratio of inertial forces to gravitational force. In Fig. 6, we attempt to determine the relationship between each number and the velocity of both phases individually.

Fig. 6 shows the relationship between pressure gradient as a function of pipeline flow distance and the Reynolds number of a two-phase flow for three values of water velocity. We can infer from the figure that the high impacts of water velocity on pressure gradients start from 2 m/s and above. These values will also result in higher Reynold's number values.

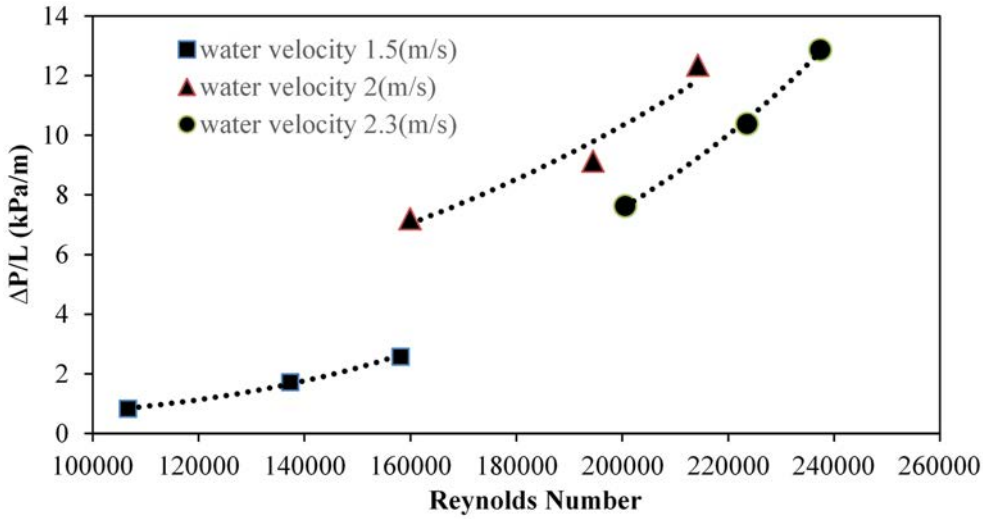

Figure 6: Pressure drop by flow distance vs. Reynold's number for three different water flow velocities.

5 CONCLUSION

In this work, the experimental set-up and computerization system provided real outcomes with only a small percentage of error in the permissible range. These outcomes highlight the advantage of using such a set-up for more applications pertaining to multiphase flow. The results show that there is about a 4 kPa pressure drop for each equivalent meter length of tube for water–CO_2 flow, while the pressure drop for water flow is about 0.4 kPa for each equivalent meter length of tube. This means that the pressure drop of water–CO_2 flow is approximately 10 times the pressure drop of water flow in the same tube diameter. This estimation can be used for future work to predict pressure drop for water–CO_2 flow applications. However, another value should be considered for pressure drop prediction, which is the ratio between pressure drop and pressure supply. In our results, this ratio is 0.17% for water flow and 0.91% for water–CO_2 flow.

ACKNOWLEDGEMENT

The authors are grateful to the Memorial University of Newfoundland for supporting this research.

REFERENCES

[1] Visser, E. et al., *Towards Hydrogen and Electricity Production with Carbon Dioxide Capture and Storage*, DYNAMIS, 2007.
[2] Nordhagen, H., Kragset, S., Berstad, T., Morin, A., Drum, C. & Munkejord. S., A new coupled fluid-structure modeling methodology for running ductile fracture. *Computers and Structures*, **94–95**, pp. 13–21, 2012.
[3] Ikeda, N., Takahashi, H., Umetsu, K. & Suzuki, T., The course of respiration and circulation in death by carbon dioxide poisoning. *Forensic Sci. Int.*, **41**(1), pp. 93–99, 1989.
[4] Zaba, C., Marcinkowski, J., Wojtyla, A., Tezyk, A., Tobolski, J. & Zaba, Z., Acute collective gas poisoning at work in a manure storage tank. *National Institute of Health*, **18**(2), pp. 448–451, 2011.
[5] Langford, N., Carbon dioxide poisoning. *Toxicol. Rev.*, **24**(4), pp. 229–235, 2005.
[6] Visser, E., Hendriks, C., Barrio, M. & Koeijer, G., Dynamis CO_2 quality recommendations. *International Journal of Greenhouse Gas Control*, **2**, pp. 478–484, 2008.
[7] Michael, J., Hill, D., Ehlig, C. & Zhu, D., *Petroleum Production Systems Text Book*, 2nd ed, 2012.
[8] Tollak, S. & Hammer, M., Depressurization of CO_2-rich mixtures in pipes: Two-phase flow modelling and comparison with experiments. *International Journal of Greenhouse Gas Control*, **37**, pp. 398–411, 2015.
[9] Chen, L., Deng, B. & Rong Zhang, X., Experimental study of trans-critical and supercritical CO_2 natural circulation flow in a closed loop. *Applied Thermal Engineering*, **59**, pp. 1–13, 2013.